energies

MDPI

Review

Problems of Powering End Devices in Wireless Networks of the Internet of Things

Andrzej Michalski [1] and Zbigniew Watral [2,*]

[1] Electrical Engineering Department, Warsaw University of Technology, 00-661 Warszawa, Poland; andrzej.michalski@ee.pw.edu.pl
[2] Faculty of Electronics, Military University of Technology, 00-908 Warszawa, Poland
* Correspondence: zbigniew.watral@wat.edu.pl

Abstract: This article presents the problems of powering wireless sensor networks operating in the structures of the Internet of Things (IoT). This issue was discussed on the example of a universal end node in IoT technology containing RFID (Radio Frequency Identification) tags. The basic methods of signal transmission in these types of networks are discussed and their impact on the basic requirements such as range, transmission speed, low energy consumption, and the maximum number of devices that can simultaneously operate in the network. The issue of low power consumption of devices used in IoT solutions is one of the main research objects. The analysis of possible communication protocols has shown that there is a possibility of effective optimization in this area. The wide range of power sources available on the market, used in nodes of wireless sensor networks, was compared. The alternative possibilities of powering the network nodes from Energy Harvesting (EH) generators are presented.

Keywords: Internet of Things; Energy Harvesting; wireless sensor network

Citation: Michalski, A.; Watral, Z. Problems of Powering End Devices in Wireless Networks of the Internet of Things. *Energies* **2021**, *14*, 2417. https://doi.org/10.3390/en14092417

Academic Editor: Federico Tramarin

Received: 2 April 2021
Accepted: 21 April 2021
Published: 23 April 2021

1. Introduction

The notion of powering wireless sensor networks operating in the structures of the Internet of Things is still an important and current issue. The recent dynamic development of IoT poses new challenges in terms of powering wireless tags used to identify objects. The possibilities of modern electronics have significantly expanded the range of parameters recorded by, for example, RFID and this, in turn, forces the need to use active tags with extended computational capabilities. Battery or electromagnetic power supplies are in many cases impossible to apply, hence the need to look for autonomous power supply methods. In most cases, Energy Harvesting is the only possible solution to this problem.

Interventional studies involving animals or humans, and other studies that require ethical approval, must list the authority that provided approval and the corresponding ethical approval code. The term "Internet of Things" was first used in 1999 by Kevin Ashton, director of the Auto-ID Center, who, along with David Brock and Sanjay Sarma, used RFID technology to identify devices connected within a single network. In 2015, the agenda of the European Commission, European Research Cluster on the Internet of Things (IERC) defined IoT as a dynamic global network infrastructure with self-configuring capabilities based on standard and interoperable communication protocols, in which the physical and virtual "things" present have an identity, physical characteristics and virtual personality, use intelligent interfaces and are seamlessly integrated with the information network [1].

A typical IoT network structure, shown in Figure 1, consists of four basic layers: the device layer with sensors, the communication layer, the data processing layer, and the analysis and inference layer.

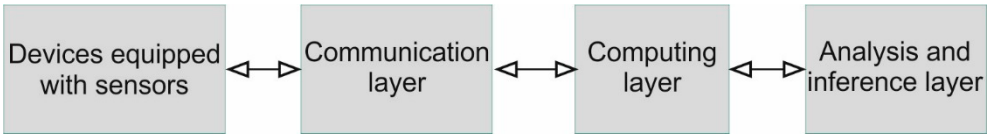

Figure 1. Simplified IoT architecture.

The first layer includes all objects equipped with sensors for electrical and non-electrical quantities, as well as transmitting and receiving devices enabling communication, receiving commands, and initial collecting and processing measurement data. The structure of a given device includes from a few to a dozen or so sensors with signal conditioning systems, transmitting and receiving systems, and a controller, creating a node in the IoT network [2]. At the input of each node, shown in Figure 2, there are sensors, and at the output, there are communication modules that provide access to the gateway.

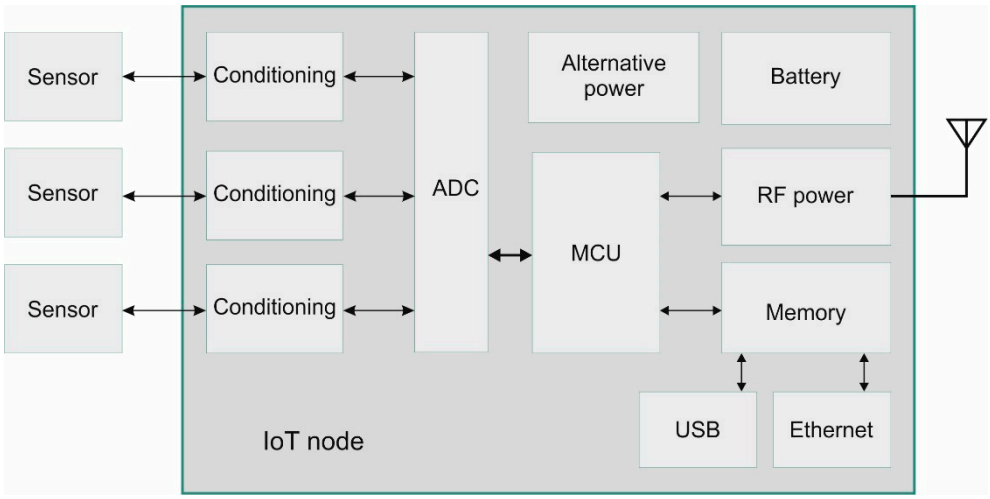

Figure 2. IoT node.

When selecting the necessary elements of the node, the main burden is on the selection of energy-saving components within the processing system. Initially, it can be assumed that the total power of a typical node should not exceed 1 W [3].

The dynamic development of applications using IoT systems has resulted in the development of specialized software platforms that enable the construction of scalable control and measurement systems using IoT technology. The concept of a platform is understood as software that will be able to ensure effective and failure-free communication between the various layers of the IoT structure. Currently, there are a number of platforms dedicated to IoT systems available on the market. The most popular are Google Cloud IoT, Microsoft Azure IoT, IBM Watson IoT, Cisco IoT Cloud Connect, Bosch IoT Suite, Oracle Integration Cloud, Comarch IoT Platform, and Hewlett Packard Enterprise [4,5].

IoT technology is clearly associated with wireless sensor networks and has diverse areas of exploitation. Indeed, it is difficult to find an area where IoT cannot be applied. Among the most popular are environmental protection, agriculture and animal husbandry, medicine, smart cities, logistics, and various industrial applications [6]. With such widespread use, it is difficult to develop a universal structure that will function properly in all environments. Each project makes a kind of compromise trying to reconcile four basic requirements: range, transmission speed, low energy consumption, and the maximum number of devices that can work simultaneously in the network.

2. Signal Transmission in IoT Networks

In the case of signal transmission in the IoT network, the most popular solution is the Wi-Fi standard–IEEE 802.11, which is available for most devices found both in everyday

use and in industrial solutions. The currently exercised standards are 802.11a, 802.11b, 802.11g, 802.11n, 802.11ac, and more recently, 802.11ax. The band used is not licensed, and the only limitation is EIRP radiation power, which, for example, for the 2.4 GHz band, is 100 mW. In practice, we encounter standards that differ in the range of frequencies used: ISM: 1–6 GHz, 5 GHz, 2.4 GHz, and the WiGig IEEE 802.11ad standard, which operates in the 60 GHz band [5,7,8]. Each of these standards differs in transmission speed and potential range.

The second very popular type of communication in the short-range area (PAN–Personal Area Network) is a family of standards defined in IEEE 802.15.1 [5], known as Bluetooth. This standard distinguishes three classes of devices with different ranges in open space (100 m, 10 m, and 1 m). In practical solutions, the most common standard is Bluetooth 4.0 + LE (Low Energy), which is characterized by very low energy consumption and a range of up to 100 m in the open area.

Another means of communication harnessed for IoT networks is mobile telephony. We distinguish five basic standards: GPRS (General Packet Radio Service), EDGE (Enhanced Data rates for *GSM* Evolution), HSDPA (High-Speed Downlink Packet Access), LTE (Long Term Evolution), and 5G. These standards provide IP connectivity through the infrastructure of the mobile operator. Apart from the obvious advantages of this type of communication, there is one major disadvantage of the necessity to use the services of a commercial operator.

An interesting and widespread means of communication in IoT networks is LoRaWAN (Long Range WAN) technology. The LoRaWAN technology has been designed to meet four very important requirements for IoT: minimum electricity demand, large network capacity, long-range and low-cost end devices. The main advantages of the LoRaWAN technology when applied to IoT are additionally the possibility of self-building own infrastructure, high security of transmitted data, and high resistance to interference. As for the disadvantages, in Poland, these are mainly low data transfer speeds, and that publicly available networks currently do not cover a large area of the country [4].

Many practical solutions apply two relatively popular wireless communication protocols, Z-Wave and ZigBee. Z-Wave is a wireless protocol with a mesh topology used to connect many devices into one network. The number of intermediary nodes in transmission is four, which allows the creation of a wireless network with a range five times greater than the range of the connection between the control panel and Z-Wave devices. This solution has one major advantage—it enables the construction of a network of sensors in a way that does not interfere with the construction infrastructure of the facilities [9].

As with Z-Wave, the ZigBee network also uses a mesh topology, with all its advantages. The ZigBee specification uses the IEEE 802.15.4 [10,11] standard, which defines the wireless transmission method. A typical structure of a Z-Wave network consists of three basic blocks: a coordinator (ZigBee Coordinator), whose task is to collect data and is a connection point for other devices; a router (ZigBee Router) ensuring data transmission from end devices to the coordinator; the end device (ZigBee End Device), which sends data to the router to which it is connected. Data sent over the network is encrypted with the symmetric AES algorithm with a key length of 128 bits. The main advantages of this technology are the relatively high level of data security and the low cost of devices. As far as the disadvantages are concerned, experts mainly mention low data transfer speed and low network capacity.

3. RFID—Universal End Node in IoT Networks

RFID tags are one example of a universal end node in IoT technology. RFID is a term for a system based on transponders used for radio identification of objects. The history of RFID technology dates back to World War II. The IFF (Identification, Friend or Foe) system, invented in Great Britain for identifying aircraft, is considered the predecessor of RFID. An early version of RFID was the predecessor of the EAS (Electronic Article Surveillance) system, introduced in the 1960s. Magnetized strips of metal attached to the

products were detected by a detector at the exit of the store, similar to today's anti-theft systems. The first RFID device, or radio transmitter with memory, was patented in 1973, in the United States, by Mario Cardullo. It was a passive tag powered by an electromagnetic signal with 16-bit memory. In 1973, the Freyman brothers demonstrated a system operating at 915 MHz, which is still used today by most UHF chips. The first fully functional RF identification system was TIRIS, introduced by Texas Instruments in the 1970s and is still operational today. Miniaturization, enhanced tag memory, and the addition of various new functionalities (e.g., measurement of temperature, humidity, and GPS) have enabled newer and newer applications [1,2].

RFID tags consist of three basic parts, an electronic system responsible for data storage and processing, as well as creating a radio signal; an antenna for receiving and sending signals; a housing, which can be in the shape of a plastic card, a thin adhesive foil, or a capsule. There are several types of RFID tags (RFID chips): active, passive, and semi-passive [2,12]. Figure 3 shows examples of passive and active RFID tags.

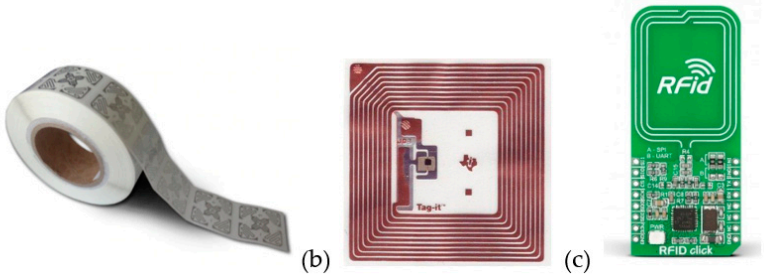

(a) (b) (c)

Figure 3. (**a**) RFID tags (TAGS), (**b**) passive, and (**c**) active [13].

The main feature of active RFID circuits is the presence of a power source that powers the RFID chip with an integrated antenna. Thanks to the antenna being powered by an internal battery, the signal sent to the reader is stronger than in other types of systems, which results in greater efficiency and accuracy of data transmission, better resistance to interference (e.g., electromagnetic or environmental), and an increased reading range up to 100 m. The disadvantages of this type of solution are larger sizes, price, and shorter operation time.

Passive RFID systems do not have their own power source, and the electric energy needed for a temporary operation is obtained from the electromagnetic field emitted by the reader. The lack of an internal power supply results in a weaker signal being cast out by the antenna, and thus a significantly shorter range (up to 10 m). However, the lack of internal power is a specific advantage of this type of RFID system. Their standard operating time is counted in years, which, as stated in [14], may even reach a half-century. An additional advantage is the low cost of production, which means that it can be treated as a replacement for barcodes and labels.

Semi-passive RFID systems are a kind of compromise between passive and active systems. The internal battery only powers the microprocessor system, and the antenna is powered, as in the case of passive systems, with the energy of the field emitted by the reader.

A typical structure of a system using RFID tags as identification elements consists of four main elements, a tag (TAG), an antenna, an RFID reader, and a database (Figure 4) [15].

Figure 4. The structure of the system using RFID tags.

There are several RFID technology standards depending on the intended use of the tags. The main difference between the standards is the operating frequency, read range, data rate, noise immunity, and error handling. Currently, communication with RFID devices is mainly within three basic radio frequency ranges: 125 kHz (LF and Unique), 13.56 MHz (HF, Mifare, and NFC), and 860–956 MHz (UHF) [2].

The frequency of 125 kHz (LF–low frequency) is exploited by the Unique and Hitag standards. Both of these standards use passive tags with a small range (max. 10 cm). The UNIQUE standard is characterized by a unique code that is written on each tag, transmits data at a speed of 2 kb/s, and is currently the most commonly used type in proximity cards. Hitag is a more technically advanced standard working within a frequency of 125 kHz. It allows writing and reading data at a speed of 4 kb/s and enables the employment of anti-collision and encoding algorithms.

The frequency of 13.56 MHz (HF–high frequency) allows the reading and writing of data at a distance of up to 1 m. It ensures stable communication between the reader and the tag, is resistant to external interference and a high speed of data reading. The HF frequency range is harnessed in systems conforming to ISO/IEC 14443 (proximity cards—they are primarily utilized for financial transactions such as automatic fare collection, bankcard activity, and high-security applications) or ISO 15693 (vicinity cards—they are primarily utilized as a contactless smart card or smart tags).

The frequency of 860–956 MHz (UHF RFID Gen2–ultra-high frequency) allows the reading and writing of data at a distance of up to 20 m at a very high speed. This standard is equipped with anti-collision procedures, and the handling of this frequency is specified in the ISO 18000-6 standard.

The main source of electricity in RFID tags are batteries (active and semi-active systems) or electromagnetic fields (passive systems). Battery power is most often applied where higher transmitter power or increased data processing requirements, or a number of connected sensors are required. In the case of battery and accumulator operation, the main problems are the need for periodic replacement and their dimensional limitations.

4. Battery and Accumulator Power Supply of IoT Nodes

Currently, a wide range of power sources is available on the commercial market, mainly galvanic cells, fuel cells, and supercapacitors. In the case of primary cells, the energy capacity level does not exceed 4.2 Wh (1.5 V, AAA size cells or less), and for 1.2 V Ni-MH rechargeable batteries, the capacity level does not go beyond 0.96 Wh. Micro fuel cells are a promising solution, but they are still in the research phase, inter alia, due to the relatively high risk of fire, which is particularly important when using many measuring nodes located in a small space. Commonly employed in emergency power and automotive systems, lead-acid batteries ($Pb0_2$) have the lowest specific power and low specific energy, which makes them heavy, and therefore they are exploited mainly in a stationary mode [16].

Portable receivers have forced the development of electrochemical sources, mainly in the direction of reducing mass and volume while maintaining high energy capacity. Thus, new nickel-cadmium (Ni-Cd), nickel-metal hydride (Ni-MH) batteries, and finally, lithium (Li-Ion) batteries have appeared.

Fuel cells accumulate energy in the form of hydrogen fuel, and the specific energy depends mainly on the type of fuel. In addition to galvanic and fuel cells, electrochemical capacitors called supercapacitors have become an increasingly important device for accumulating electricity. They are characterized by high specific power and, unfortunately, low specific energy.

This complementarity of features between electrochemical capacitors and galvanic cells suggests the cooperation of these slightly different electricity stores. Storing energy in the form of electricity is supported by the ease of transport, distribution and regulation, and the conversion of electricity to the parameters necessary for use. Its main disadvantage is that it is difficult to store, so very often electricity is generated when it is needed. If electrical energy is stored, it can be stored directly in the form of electrostatic charge in capacitors and supercapacitors between the electrode and electrolyte or in battery galvanic cells through the use of chemical transformation [17]. Battery cells last a long time but release energy slowly, while supercapacitors can take and deliver more charge in less time. In the case of battery cells, electrical energy is converted into chemical reaction energy. The phenomenon of electricity storage in electrochemical devices is the basis of the operation of an electrochemical capacitor. Unlike battery cells, supercapacitors do not undergo typical oxidation and reduction reactions because there is no chemical reaction [18]. Energy storage is mainly subject to electrostatic forces. The polarity of the electrodes (negative and positive) is based on the reversible adsorption of electrolyte ions on the electrodes. At the interface between the electrode and the electrolyte solution, the so-called Electrical Double Layer (EDL) is formed [19]. Supercapacitors are characterized by high power density, high capacity, and efficiency at the order of 90%. They can be charged and discharged many times, also with the use of very high currents. The charging process is very fast compared to batteries. Supercapacitors have a very long service life and can be discharged to zero without any negative impact. In addition, they are maintenance-free. The disadvantages of this type of electricity storage include quick self-discharge and variable voltage on the terminals resulting from the exponential drop during discharge. Due to their structure, two types of supercapacitors can be distinguished: folded and wound. The former have lower power density and low losses when loaded with high currents [20–22].

Based on the above characteristics, it can be concluded that supercapacitors are perfectly suited for working with renewable energy sources. Energy storage in the IoT system can take place in an electrochemical capacitor with a very large capacity due to its expected large number of operating cycles. The energy storage device will be exposed to constant charging and discharging, which in the case of a battery cell will limit its lifetime and make it necessary to replace it sooner. In addition, the energy battery may be completely discharged when the station is not in use. Such a situation may lead to irreversible changes in battery cells, resulting in deterioration of their parameters, especially their capacity, and internal resistance.

An example of a supercapacitor available on the market is the electrochemical EDLCs electrochemical double-layer capacitor PHV-5R4V505-R by Eaton -Electronics Division USA, with a capacity of 5F in a cylindrical housing with dimensions of $10.5 \times 20.8 \times 32$ mm. The operating voltage is 5.4 V, and the internal series resistance (ESR) is 0.07 Ω.

With regard to the issue of electrical energy storage, it can be, therefore, stated that electrochemical capacitors are adapted to the process of rapid energy accumulation and return, and at the same time, they can withstand a much greater number of charge/discharge cycles than battery cells [23]. However, they are able to store much less electricity than battery cells or fuel cells. A comparison of the basic features of electrochemical capacitors and battery cells shows that these devices can complement each other. The supercapacitor, thanks to its excellent dynamic parameters, can become a buffer protecting the battery cell against excessive load, while the battery cell ensures that such hybrid energy storage has a long operation time. It is for these reasons that supercapacitors are very often combined with chemical cells. Table 1 shows the efficiency of electricity sources used to power end devices in IoT networks [24].

Table 1. Efficiency of electricity sources used to power end devices in IoT networks.

Type	Capacity (Ah)	Rated Voltage (V)	Working Temperature (°C)	Specific Energy (Wh/kg)	Number of Cycles
Lead-Acid	1.3	2	20–60	30–50	500–1000
Li poli-carbon	0.025–5	3	20–60	100–250	-
NiCd	1.1	1.2	40–70	50–60	$10–20 \times 10^3$
MnO_2Li	0.3–5	3	20–60	280	1000–2000
Li-Ion	0.74	3.6	30–45	75–200	$10^3–10^5$
$LiSOCL_2$	0.025–40	3.6	40–85	350	-
MnO_2	0.617	1.65	20–60	300–610	-
NiMH	2.5	1.2	20–40	60–70	$10^3–20 \times 10^3$
LiO_2S	0.025–40	3	60–85	500–700	-

Thin Film Batteries (TFB) are increasingly used for energy storage. TFB batteries are most often produced with the use of techniques typical for thin-film structures; for example, batteries produced by ORNL are produced with the use of sequentially applied thin layers on a solid substrate [3]. A cross-sectional view of such a battery, adapted from [25] is shown in Figure 5.

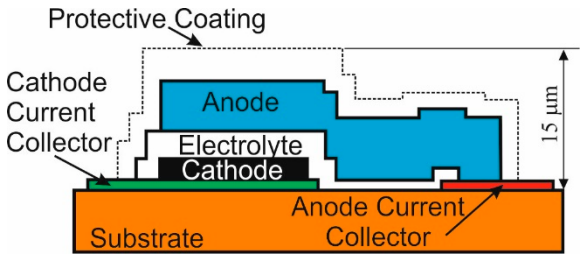

Figure 5. An example of a cross-section of a thin-film battery.

Each layer is from a few to a dozen or so µm thick. The substrate on which the active layers are applied can be silicon, mica, alumina, or a metal foil. Due to their thinness, TFB batteries are flexible and can adapt to the surface on which they are placed. The typical surface of such a battery is in the order of several cm^2 with a capacity not exceeding 10 mAh. The materials from which the anode and cathode are made are selected depending on the purpose of such a battery (e.g., metallic lithium). The biggest technological challenge is the solid electrolyte layer. Different solutions are used depending on the manufacturer; for example, Oak Ridge National Laboratory uses glassy lithium phosphorus oxynitride as the electrolyte layer, now known as Lipon, which is sputtered on the cathode.

Recently, dynamic development of printed batteries has been observed. This is due to the wide availability of 2D and 3D printers. These batteries are thin, flexible, cheap, and more environmentally friendly, which results in an increasing number of applications each year, such as smart cards, radio frequency identification, portable medical diagnostic systems, and various sensors. 3D printing technology is particularly effective in this area [26].

5. Energy Harvesting Applied to Power IoT End Nodes

The issue of low power consumption of devices used in IoT solutions is one of the main research objects of today. The analysis of possible communication protocols has shown that there is a possibility of effective optimization in this area.

In wireless sensor networks, the energy demand of a single autonomous node depends on the current operating mode. In standby mode, the demand for electricity usually does not exceed a dozen or so µW, and during measurement, it does not exceed 100 µW. The

greatest demand occurs during the transmission of information and ranges from 0.1 to 1 mW depending on the type of transmission algorithm or the communication protocol used. Such values of energy demand clearly indicate the possibility of using EH generators as the only sources of power for the autonomous measuring node. The densities of obtained energy range from single $\mu W/cm^2$ in the case of using electromagnetic phenomena to 1500 $\mu W/cm^2$ in the case of applying photovoltaic phenomena [2,14,27].

The main sources of energy employed in these types of generators are the natural environment of man and the man himself. In the case of humans, two types of energy are primarily used: kinetic and thermal, and the environment makes it possible to harness, apart from the previously mentioned, radiation energy as well. Different phenomena are exploited in each of these types of energy. In the case of kinetic energy, these phenomena are piezoelectric, electromagnetic, and electrostatic. In the case of thermal energy, thermoelectric phenomena, and in the case of radiation energy, the phenomenon of photovoltaic and RF radiation. These phenomena have very different energy efficiencies. Table 2 presents a summary of the obtained average energy densities for the phenomena most frequently used in EH [3,24].

Table 2. List of average energy densities for the discussed phenomena.

Types of EH Energy Source	EH Generators	Power Density (Maximum)
Solar and electromagnetic radiation	solar panels for solar radiation	1500 $\mu W/cm^2$ (at the intensity of radiation 1000 W/m^2)
	RF antennas for electromagnetic waves	20 mW
Kinetic	wind turbines	3.5 mW/cm^2
	piezoelectric generators	500 $\mu W/cm^2$
	electromagnetic generators	4.0 $\mu W/cm^2$
	electrostatic generators	3.5 $\mu W/cm^2$
Thermoelectric	Peltier cells	40 $\mu W/cm^2$; 100 $\mu W/cm^2$ (at the gradient 5 °C)

When applied for powering hybrid sources, an example of which can be a combination of several EH generators with energy storage, we create the possibility of obtaining sufficient energy without the inconvenience associated with the need to periodically replace galvanic cells [28,29]. Among the EH generators, the most important are those that exploit kinetic, thermal, and radiation energy. The phenomena underlying the operation of EH generators include piezoelectric, electromagnetic, electromagnetic radiation in the RF range, electrostatic, thermoelectric, and photovoltaic [3].

The classic piezoelectric phenomenon consists of the polarization of a crystal in a specific direction, caused by mechanical deformation, or vice versa, by deformation under the influence of an external electric field. This phenomenon is explained by the displacement of ions in the crystal lattice, which creates an internal electric field in the crystal. The higher the degree of symmetry of the crystal, the fewer directions of polarization. This phenomenon does not occur in crystals with a center of symmetry. Within a certain range of mechanical deformations, there is linearity between the resulting electric field strength and the deformation. The phenomenon of piezoelectricity was discovered in 1880 by Peter and Jacob Curie. They noticed that quartz changes its dimensions under the influence of an electric field and vice versa; it generated an electric charge due to mechanical deformation. In 1881, G. Lippmann theoretically predicted the existence of the reverse piezoelectric phenomenon. He assumed that an electric voltage applied to some surfaces of a quartz crystal should cause its mechanical deformation. In the same year, the Curie brothers experimentally confirmed Lippmann's hypothesis. The piezoelectric phenomenon was, for

the first time, exercised practically in 1920 by Langevin, who built a quartz transmitter and receiver for underwater sounds—the first sonar [2,30,31].

An example of a generator that harnesses the piezoelectric effect is shown in Figure 6. These systems are adapted for working in a wide frequency spectrum of forced vibrations. Electromagnetic EH generators are a group of devices that use the effects resulting from the interaction of a magnetic field, an electric field, and most often, one of the motion parameters. The effect of such interaction is induced electromotive force.

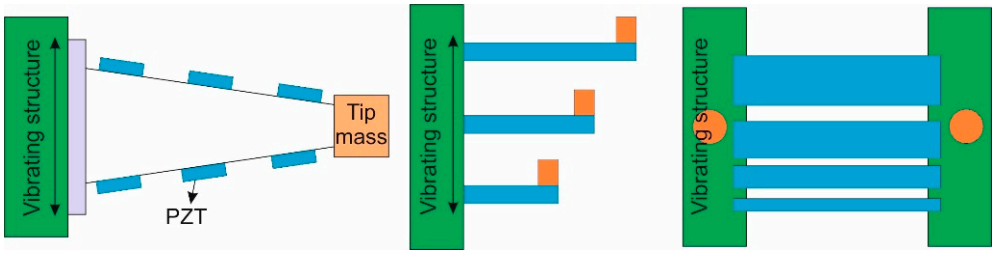

Figure 6. Finger-like systems of elastic beams with an extended spectrum of resonance frequencies using the piezoelectric effect (PZT-Lead Zirconate Titanate piezoelectric materials).

In 1831, Michael Faraday showed that if a closed electric circuit (conductor) is placed in a magnetic field and there is a relative change in time of this field in relation to the circuit placed in it, then an electromotive force will appear in this circuit, which is a function of the parameters of the electric circuit and the rate of change of the magnetic field. In all generator systems using the electromagnetic effect, there is a permanent magnet as a source of a constant magnetic field and a coil as an electrical signal detector. The relative movement that must occur between the coil and the magnet is caused by natural phenomena, e.g., vibrations to which the generator structure is subjected. From the generator's efficiency point of view, it does not matter which element, coil, or magnet is moved and which is fixed. Most EH electromagnetic generator designs use a resilient magnet or coil suspension. This is most often done with the help of classic mechanical solutions. Figure 7 is an illustration of an EH electromagnetic generator using an elastic beam.

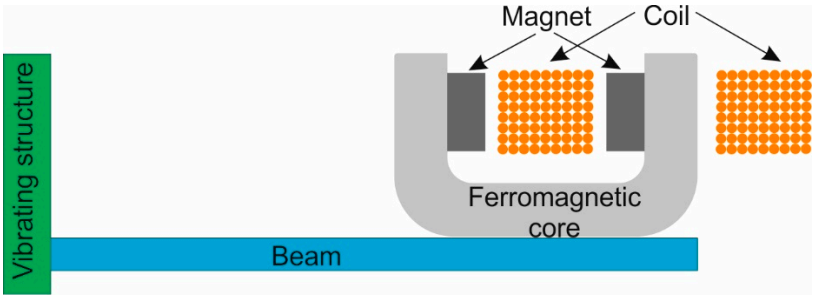

Figure 7. An electromagnetic EH generator using an elastic beam.

The issue of obtaining electricity from electromagnetic radiation in the field of RF has been studied for over 50 years. The scale of this type of undertaking is very diverse, ranging from wireless powering a helicopter through powering dust sensors and ending with powering an eyeball pressure measurement system installed in contact lenses. Currently, most works are carried out in two areas: providing power to mobile devices using RF radiation in the 935 MHz (GSM) to 2.4 GHz (Wi-Fi) band, where the antenna size does not exceed several dozen square centimeters and providing power for active RFID systems. These systems have many applications, ranging from logistical movement of goods, to kinaesthetic patient tracking in hospitals. RFID systems are slowly replacing the bar codes currently used to mark goods. The presence of RF radiation sources in the natural environment of man is common. All kinds of RF signal transmitters are an invaluable source of electricity. Energy from GSM, Wi-Fi, TV, and radio transmitters is most often

used. A planar coil that serves as an antenna for electromagnetic energy transfer in the RF range is seen in Figure 8 [32].

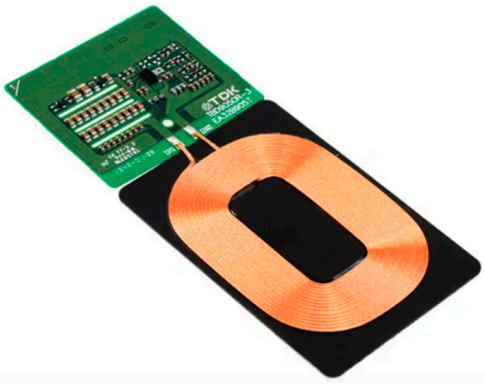

Figure 8. A planar coil used for electromagnetic energy transfer in the RF range.

The basis of the operation of electrostatic generators is the conversion of forces causing the movement of electrically conductive parts (capacitor facings) in an electric field into an electrical signal. There are two types of generators: generators using air dielectric capacitors and generators with electrets. In the former, the conversion consists of the specific charging and discharging of the capacitor while changing its configuration. In generators of the second type, there is a direct conversion of the electrode movement into electricity without the need to charge the capacitor. A characteristic feature of generators with an air condenser is the need to provide an external source of energy so as to initiate the process of converting mechanical energy into electricity. The typical structure of such a generator is based on a flat capacitor with an air dielectric. Two types of generators are distinguished: flat capacitors operating with a constant charge; comb capacitors operating with constant voltage [3]. Figure 9 shows an electrostatic generator of the MST technology-type, operating in a constant voltage system.

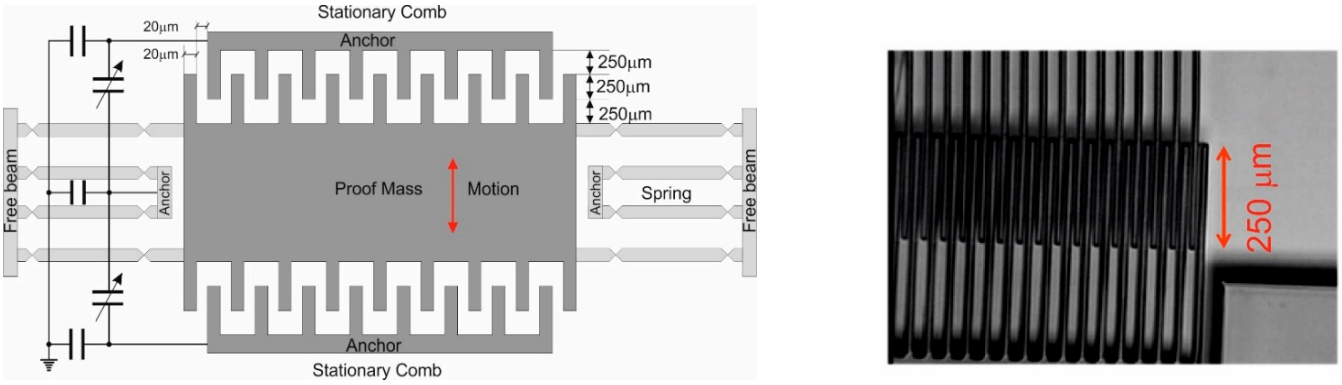

(**a**) (**b**)

Figure 9. Electrostatic generator built according to MST technology, operating in a constant voltage system; (**a**) generator diagram; (**b**) actual view of the comb capacitor.

Thermoelectric generators are small and contain no moving parts, and in addition, they are resistant to mechanical damage and are quiet, which makes them ideal micro sources of electricity for a wide range of applications, e.g., medical. The most famous example of the employment of thermoelectric generators is in the hand watches of Seiko and Citizen. The generator found in the Seiko watch, using a temperature gradient of 1.5 °C, produces 22 µW of electrical power at a voltage of 300 mV. These values are sufficient for the undisturbed operation of the watch.

The history of the thermoelectric phenomenon dates back to the 1820s. The first to discover this was Thomas Johann Seebeck. He observed that a compass needle moves when it is located near the junction of two different metals placed at different temperatures. Seebeck's original interpretation of this phenomenon as a magnetic one was wrong. The correct interpretation was presented a little later by H.C. Oersted and J. Cumming, who attributed the observed effect to electrical properties. Another person who made a significant contribution to the full elucidation of the thermoelectric effect was J.C. Peltier, who discovered in 1834 that the temperature at the junction of two conductors changes when connected to an electric current source. He also noticed that the temperatures of the metals differed at their ends and that the current flow was absorbing heat at one end and releasing at the other. As with Seebeck, Peltier's original interpretation of this phenomenon was wrong.

The Peltier effect was correctly interpreted only in 1838 by Emil Lenz by means of the simple experiment of placing a drop of water at the junction of two conductors. The phenomenon of freezing and then thawing of water due to the change in the polarity of the current flowing through the junction correctly illustrated the Peltier effect. In 1854, William Thomson defined the Peltier and Seebeck phenomena as unified. Due to the low energy efficiency of the discovered phenomena, they did not attract much attention, and it was not until the middle of the twentieth century, when semiconductor materials began to be used, that the Seebeck effect became of interest once more.

At the beginning of the twenty-first century, there was a significant breakthrough in research on thermoelectric materials, which resulted in the development of thermoelectric materials with a thermoelectric figure of merit ZTz T {\displaystyle zT}, value of around 2. The basis of the thermoelectric generator operation is the Seebeck effect, which describes the migration of mobile electric charge carriers in the material as a result of subjecting this material to a non-zero gradient temperature. This effect is caused by the superimposition of two phenomena. The first results from the diffusion of electrons in the n-type material and holes in the p-type material caused by different concentrations of high-energy current carriers at both ends of the material. The "warmer" carriers diffuse in the direction of the "cold" junction, and the "colder" carriers in the opposite direction. Due to the scattering of the migrating carriers, carriers with higher energies diffuse faster. This creates an electric field that counteracts this movement. As a result, there is a thermoelectric voltage component in the circuit related to the diffusion of carriers.

The second cause of the thermoelectric force is related to the phonon drift caused by the temperature gradient existing along the conductor. The migration of phonons causes their collisions with charge carriers, as a result of which part of the kinetic energy of the phonons is transferred to the charge carriers. As a result of the excitation of the charge carriers, they flow towards the end with the lower temperature. Charges accumulated at the "cold" end create a "phonon" component of the thermoelectric force. Figure 10 shows the construction of a thermoelectric EH generator [33].

The basis of the operation of photovoltaic generators is the internal photoelectric effect. The internal photoelectric effect consists of the encountered electrons taking over all the energy of the light wave falling on the body. The cell contains a reverse-biased p-n junction in which incident photons with energy greater than the width of the semiconductor gap are absorbed inside the barrier layer, generating an electron-hole pair. The electric field of the junction causes the accumulation of electrons in the n-type region and holes in the p-type region, respectively. As a result, an external electrical voltage is generated at the junction. The electrons flowing into the p region recombine with the holes, generating a photocurrent, the value of which is directly proportional to the light intensity and does not depend on the cell's voltage. The efficiency of light radiation energy conversion into electricity is closely related to weather conditions, the angle of sunlight, or cloud cover. These factors are related to the climate and latitude of the region in which the device is located. In regions with a temperate climate, insolation ranges on average from 1–5 $MJ/m^2/day$ in winter and up to 25 $MJ/m^2/day$ in summer. The materials from which the photovoltaic cells are

built should be characterized by high efficiency and low cost of energy conversion. In practice, three groups of materials are used: inorganic, organic, and DSSC (Dye-Sensitized Solar Cells).

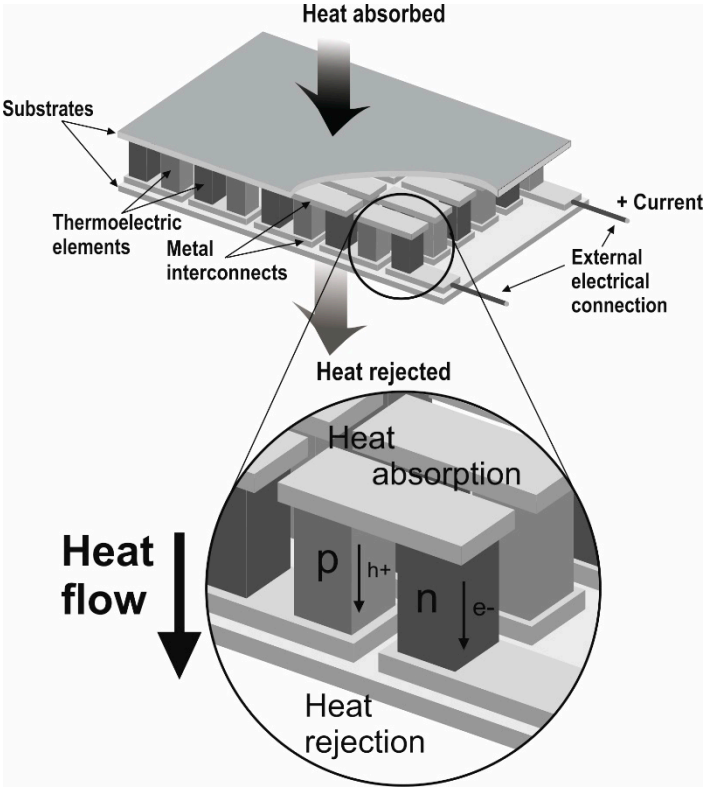

Figure 10. Construction of a thermoelectric EH generator.

The most commonly used inorganic materials are polycrystalline silicon, microcrystalline silicon, indium-copper diselenide (CIS), gallium arsenide, and indium phosphate. All these materials have a bandgap between 1.1 eV and 1.7 eV. The optimal bandwidth for the photovoltaic energy conversion of a single PV cell junction is 1.5 eV, and therefore inorganic materials meet this requirement. Organic materials are cheaper than silicon, and the photovoltaic effect occurring in them is based on the flow of an electron from a semiconductor conjugated donor-type polymer to a conjugated acceptor-type polymer. Semiconductor polymers have a lower dielectric constant but also a higher expiration constant than inorganic materials. Moreover, due to the low mobility of the carrier, the optimum thickness of most polymer photovoltaic cells is around 100 nm.

The latest development is the DSSC photovoltaic cell. This was invented by Michael Gratzel and Brian O'Regan in 1991. DSSC cells represent the third generation of photovoltaic cells based on organic compounds. In these, there is no p-n junction typical for the first and second generations. Figure 11 shows a measurement node that uses a photovoltaic panel as a source of electricity.

Figure 11. Measurement node using a photovoltaic panel [34].

Due to the need to improve the efficiency of EH generators, hybrid systems are increasingly harnessed, i.e., those that use more than one phenomenon to generate electricity. In practical solutions, there are two types of hybrids: the first uses various phenomena in the mechanical structure of the generator, the second combines various phenomena at the level of the energy management system and its accumulation. The most typical hybrid system, belonging to the first group, is a structure that employs a typical spring beam made of elastic material, on which typical piezoelectric elements (ceramic or foil) are glued. The function of the seismic mass at the end of the beam is performed by a permanent magnet placed inside the coil. As a result of the forced free vibrations of the beam, mechanical stresses appear in it, which results in two effects of electricity generation: the typical piezoelectric effect and the electromagnetic effect caused by the movement of the magnet inside the coil. This structure is characterized by high efficiency in a wide range of vibration frequencies. The piezoelectric system is more efficient at higher vibration frequencies, and the electromagnetic system is more efficient at lower frequencies. Figure 12 illustrates a hybrid EH generator that uses the piezoelectric and electromagnetic effects [35,36].

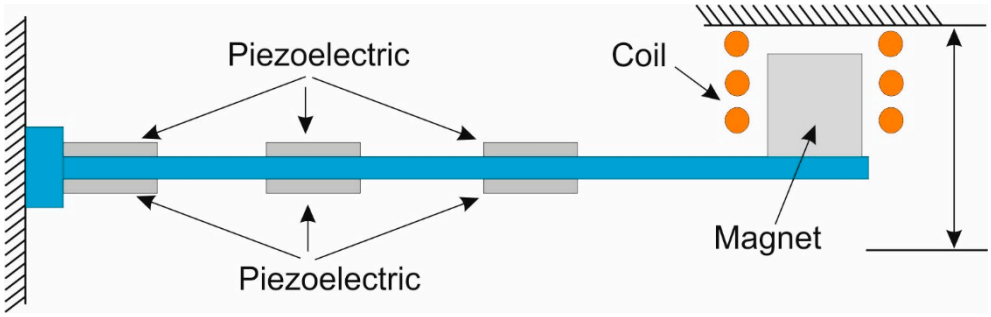

Figure 12. A hybrid EH generator exploiting the piezoelectric and electromagnetic effects.

Currently, there are a number of dedicated power supply systems using EH generators on the market. Among them, the two most typical ones can be distinguished as follows. Sol Chip SCC-S433 (Sol Chip, USA)—this system applies the phenomenon of energy being obtained through solar radiation. The system has an implemented energy storage that ensures fully autonomous operation of the node. The built-in transmitter provides communication at 433 MHz with a range of up to 1500 m. Due to its advantages, the system is widely used both in smart city structures and in agriculture. In contrast, ReVibe (Revibeenergy, Sweden) is a generator based on the conversion of the energy of mechanical

vibrations into electricity. The efficiency is so great that it can power several standard sensors. The range of processed vibrations is relatively wide, from 15 to 100 Hz, and the achievable capacities are up to 150 mW.

6. Summary

Upon analyzing the dynamic development of IoT technology in recent years, it can be clearly stated that this technology entails the development of other areas of life. At present, it is difficult to find a field of life in which IoT technology is not or cannot be applied. The constant pursuit of miniaturization of measuring devices and ensuring their maintenance-free operation has resulted in the development of alternative power sources. The emergence of Energy Harvesting technology and its further development is a typical scientific response to market demands. While the energy conversion itself is relatively well developed, the same cannot be said about efficient methods of its storage. The presented analysis of electricity storage sources has shown that the existing solutions do not fully meet the expectations of users. However, in this matter, significant progress has been observed in the last five years.

Author Contributions: A.M. developed: the general concept and draft of the article, an introduction to the subject, signal transmission in IoT Network, RFID-universal End Node in IoT Networks and a summary. Z.W. developed issues related to: battery and accumulator Power Supply of IoT Nodes, Energy Harvesting Applied to Power IoT End Nodes and references. Both authors have read and agreed to the published version of the manuscript.

Funding: This work was financed by Military University of Technology under research project UGB 22-850.

Institutional Review Board Statement: Not applicable.

Data Availability Statement: Not applicable.

Conflicts of Interest: The authors declare no conflict of interest. The funders had no role in the design of the study; in the collection, analyses, or interpretation of data; in the writing of the manuscript, or in the decision to publish the results.

References

1. Ashton, K. That 'internet of things' thing. *RFID J.* **2009**, *22*, 97–114.
2. Michalski, A.; Watral, Z. Internet Rzeczy—Narzędzie współczesnej metrologii. In *Wybrane Aspekty Internetu Rzeczy w Zastosowaniach Metrologicznych*; Wojskowa Akademia Techniczna: Warsaw, Poland, 2020; pp. 9–28.
3. Michalski, A.; Watral, Z.; Jakubowski, J. Energy Harvesting—Realna możliwość alternatywnego zasilania bezprzewodowych sieci sensorów. In *Wybrane aspekty zastosowania technologii „Energy Harvesting" w Zasilaniu Bezprzewodowych Sieci Sensorowych*; Wojskowa Akademia Techniczna: Wasrsaw, Poland, 2017; pp. 39–88.
4. Wiszniewski, Ł. Wykorzystanie technologii LoRaWAN w bezprzewodowych systemach IoT. In *Wybrane Aspekty Internetu Rzeczy w Zastosowaniach Metrologicznych*; Wojskowa Akademia Techniczna: Warsaw, Poland, 2020; pp. 29–58.
5. Sieczkowski, K. Jednoukładowe komputery SBC w zastosowaniach IoT. In *Wybrane Aspekty Internetu Rzeczy w Zastosowaniach Metrologicznych*; Wojskowa Akademia Techniczna: Warsaw, Poland, 2020; pp. 59–92.
6. Satish, G.N.; Varma, P.S. Internet of Things—Opportunities, Applications and Challenges in the Prospective Smart World. *Int. J. Comput. Sci. Inf. Technol.* **2017**, *4*, 8–16.
7. IEEE802.11ad. Available online: https://standards.ieee.org/search-results.html?q=IEEE20802.11ad (accessed on 31 March 2021).
8. IEEE 802.15.1. Available online: https://standards.ieee.org/search-results (accessed on 31 March 2021).
9. Z-Wave Alliance. Available online: https://z-wavealliance.org/ (accessed on 31 March 2021).
10. Wiszniewski, Ł. Suitability of LoRaWAN Technology for the Development of Maritime Applications. *Task Q.* **2018**, *22*, 4.
11. Park, C.; Chou, P.H. Ambimax: Autonomous energy harvesting platform for multi-supply wireless sensor nodes. In Proceedings of the 3rd Annual Communications Society on Sensor and Ad Hoc Communications and Networks, Reston, VA, USA, 25–28 September 2006; Volume 1, pp. 168–177.
12. Tagi RFID—Zbliżeniowe Chipy Radiowe, PWSK. 2020. Available online: https://www.pwsk.pl/rfid/tagi-rfid/ (accessed on 12 November 2020).
13. RFID Technologies. Available online: https://automatykaonline.pl/Artykuly/Montaz-i-transport/technologie-rfid-wprowadzenie (accessed on 31 March 2021).

14. Sigrist, L.; Gomez, A.; Lim, R.; Lippuner, S.; Leubin, M.; Thiele, L. Measurement and validation of energy harvesting IoT devices. In Proceedings of the Design, Automation & Test in Europe Conference & Exhibition, Lausanne, Switzerland, 27–31 March 2017; pp. 1159–1164.
15. Radio Frequency Identification (RFID) Tags and Reader Antennas Based on Conjugate Matching and Metamaterial Concepts. Available online: https://www.tdx.cat/bitstream/handle/10803/133356/gzg1de1.pdf?sequence=1 (accessed on 10 March 2021).
16. Gene, Y.; Corey, A.; Yuxi, M.; Myoungseok, L.; Evan, H.; Dahyun, O.; Dongkyu, L. Advances in Materials Design for All-Solid-state batteries: From Bulk to Thin Films. *Energ. Appl. Sci.* **2020**, *10*, 4727.
17. Gilbert, J.M.; Balouchi, F. Comparison of energy harvesting systems for wireless sensor networks. *Int. J. Autom. Comput.* **2008**, *5*, 334–347. [CrossRef]
18. Simjee, F.; Chou, P.H. Everlast: Long-life, supercapacitor-operated wireless sensor node. In Proceedings of the International Symposium on Low Power Electronics and Design, Tegernsee, Germany, 4–6 October 2006; pp. 197–202.
19. Prauzek, M.; Konecny, J.; Borova, M.; Janosova, K.; Hlavica, J.; Musilek, P. Energy harvesting sources, storage devices and system topologies for environmental wireless sensor networks: A review. *Sensors* **2018**, *18*, 2446. [CrossRef] [PubMed]
20. Habibzadeh, M.; Hassanalieragh, M.; Ishikawa, A.; Soyata, T.; Sharma, G. Hybrid solar-wind energy harvesting for embedded applications: Supercapacitor-based system architectures and design tradeoffs. *IEEE Circuits Syst. Mag.* **2017**, *17*, 29–63. [CrossRef]
21. Zhang, C.; Wei, Y.L.; Cao, P.F.; Lin, M.C. Energy storage system: Current studies on batteries and power condition system. *Renew. Sustain. Energy Rev.* **2018**, *82*, 3091–3106. [CrossRef]
22. Kadirvel, K.; Ramadass, Y.; Lyles, U.; Carpenter, J.; Ivanov, V.; McNeil, V.; Chandrakasan, A.; Lum-Shue-Chan, B. A 330nA energy-harvesting charger with battery management for solar and thermoelectric energy harvesting. In Proceedings of the International Solid-State Circuits Conference, San Francisco, CA, USA, 19–23 February 2012; pp. 106–108.
23. Libich, J.; Máca, J.; Vondrák, J.; Cech, O.; Sedlaríková, M. Supercapacitors: Properties and applications. *J. Energy Storage* **2018**, *17*, 224–227. [CrossRef]
24. Elahi, H.; Munir, K.; Eugeni, M.; Atek, S.; Gaudenzi, P. Energy harvesting towards the self-powered IoT devices. *Energis* **2020**, *13*, 5528. [CrossRef]
25. Priya, S.; Inman, D. *Energy Harvesting Technologies*; Springer: New York, NY, USA, 2009.
26. Costa, C.M.; Gonçalves, R.; Lanceros-Méndez, S. Recent advances and future challenges in printed batteries. *Energy Storage Mater.* **2020**, *28*, 216–234. [CrossRef]
27. Li, H.; Zhang, G.; Ma, R.; You, Z. Design and experimental evaluation on an advanced multisource energy harvesting system for wireless sensor nodes. *Sci. World J.* **2014**. [CrossRef] [PubMed]
28. Chenglong, S.; Heejun, R.; Taekyung, K.; Wonjun, L. Multisource Wireless Energy Harvesting-based Medium Access Control for Rechargeable Sensors. *IEEE Trans. Consum. Electron.* **2016**, *62*, 119–127.
29. Chenglong, S.; Heejun, R.; Wonjun, L. Next-generation RF-powered networks for Internet of Things: Architecture and research perspectives. *J. Netw. Comput. Appl.* **2018**, *123*, 23–31.
30. Elahi, H.; Eugeni, M.; Gaudenzi, P. A review on mechanisms for piezoelectric-based energy harvesters. *Energies* **2018**, *11*, 1850. [CrossRef]
31. Chew, Z.J.; Zhu, M. Combined power extraction with adaptive power management module for increased piezoelectric energy harvesting to power wireless sensor nodes. *IEEE Sens.* **2016**, 1–3. [CrossRef]
32. Jon Gabay, RF Energy Harvesting: Batteries Not Included. Available online: https://www.digikey.pl/pl/articles/rf-energy-harvesting-batteries-not-included (accessed on 10 March 2021).
33. Sodano, H.; Dereux, R.; Simmers, G.; Inman, D. Power harvesting using thermal gradients for recharging batteries. In Proceedings of the 15th International Conference on Adaptive Structures and Technologies, Bar Harbor, ME, USA, 24–27 October 2004; pp. 25–27.
34. Shenoy, P.; Ganesan, D.; Irwin, D.; Gummeson, J.; Sharma, N.; Somerville, T.; Rivernet, A. Wireless Sensor Network for Remote Monitoring of Riverbed Ecosystems. 2016. Available online: http://sensors.cs.umass.edu/projects/rivernet/ (accessed on 1 February 2021).
35. Yang, K.; Wang, J.; Yurchenko, D. A double-beam piezo-magneto-elastic wind energy harvester for improving the galloping-based energy harvesting. *Appl. Phys. Lett.* **2019**, *115*, 193901. [CrossRef]
36. Zamacola Alcalde, G.; Quiterio Gómez Muñoz, C.; García Marquez, F.P. Energy Harvesting and Piezoelectric Transducers. *Energies Appl. Sci.* **2020**, *10*, 5951.